Agile Digital Detector for RFI Mitigation

Sidharth Misra, Christopher Ruf and Roger De Roo

Abstract—A new type of microwave radiometer detector has been developed that is capable of identifying low level Radio Frequency Interference (RFI) and of reducing or eliminating its effect on the measured brightness temperature. The Agile Digital Detector (ADD) can discriminate between RFI and natural thermal emission signals by directly measuring other moments of the signal than the variance that is traditionally measured. ADD performance has been experimentally verified in two field deployments, one while connected to a ground based L-Band radiometer operating near an ARSR-1 commercial air traffic control radar and the other while connected to an airborne C-Band radiometer (the NOAA/ETL PSR) installed on a NASA WB-57 flying over major urban centers. The ADD digitizes its pre-detection radiometer signal, performs digital sub band filtering, and then measures the first four moments of the signal's probability density function for each sub band. The second central moment reproduces the square law output of a conventional analog detector. Algorithms that utilize higher order moments are used to detect the presence of RFI.

***Index Terms*—microwave radiometer, radio frequency interference**

I. Introduction

Numerous studies have revealed that space borne microwave radiometers are subject to detrimental Radio Frequency Interference (RFI), particularly at L- and C-Band [1, 2, 3]. Previous analog and digital signal processing-based algorithms have been developed for RFI mitigation which are based on the detection of anomalous spikes in the power spectrum over narrow frequency bands [4, 5]. Such approaches will in general tend to have more trouble detecting low level or intermittent RFI. The Agile Digital Detector (ADD) is a digital signal processing radiometer detector that uses an alternative approach to RFI detection and mitigation. High order moments of the received signal are detected, from which characteristics of the probability distribution of its amplitude can be estimated. For a signal generated by thermal emission alone, the amplitude is gaussian distributed. The presence of non-gaussian distributed RFI can be detected by its influence on the high order moments. ADD performance has been empirically verified during preliminary ground based field trials [6]. Preliminary results obtained during a subsequent airborne field trial are presented below. Some statistical characteristics are also presented of the algorithm with which the presence of RFI is detected.

Manuscript received March 2, 2006.

S. Misra, C. Ruf and R. De Roo are with the Atmospheric, Oceanic and Space Sciences Department, University of Michigan, Ann Arbor, MI, 48103 USA (e-mail: cruf@umich.edu).

II. Principle of kurtosis-based RFI detection in microwave radiometry

The signal detected by a microwave radiometer is primarily from natural thermal emission as well as thermal noise generated by the hardware. The PDF of the amplitude of this signal is gaussian distributed. This property can be utilized when detecting the presence of RFI [6].

The RFI detection algorithm makes use of the generating function for higher order moments of a gaussian distribution, given by

$$m_n = \left\langle (x - < x >)^n \right\rangle = 1 \cdot 3 \cdot .... \cdot (n-1)\sigma^n \qquad (1)$$

where σ is the standard deviation of x. In case of a gaussian distributed signal, higher order moments are uniquely determined by the standard deviation. The kurtosis of x is defined as

$$R = \frac{m_4}{m_2^2} \qquad (2)$$

For a gaussian distributed signal, the kurtosis is always equal to 3, independent of σ. In case the signal is corrupted by RFI, the amplitude probability may deviate from a gaussian distribution and the value of the kurtosis may deviate from 3.

III. Kurtosis in the presence of pulsed sinusoidal RFI

The kurtosis may change in the presence of RFI. Here we characterize the behavior of the kurtosis in the presence of a radar-like source of RFI. Assume that the RFI can be modeled as a pulsed sinusoid with a duty cycle *n* and amplitude *A*. We require the probability distribution of both the thermal emission and the RFI signals. In our case, even though the RFI is deterministic in nature, we consider its amplitude histogram as an equivalent probability distribution. The probability distribution functions for the thermal emission and RFI signals are respectively represented by g(x) and f(x)

$$g(x) = \frac{1}{\sigma\sqrt{2\pi}} e^{\frac{-x^2}{2\sigma^2}} \qquad (3)$$

$$f(x) = (1-n)\delta(x) + \frac{n}{\pi\sqrt{A^2 - x^2}} \tag{4}$$

Because the two signals can be considered statistically independent, the probability distribution of the composite signal is given by a normalized version of the convolution of the above two equations, or

$$r(x) = f(x) * g(x) \tag{5}$$

In order to calculate the kurtosis, we require the first four moments of the resultant signal. Derivation of the moments of the resultant signal is aided by expansion in terms of the moments of the individual signals, according to

$$m_1^{g+f} = m_1^g + m_1^f \tag{6}$$

$$m_2^{g+f} = m_2^g + 2m_1^g m_1^f + m_2^f \tag{7}$$

$$m_3^{g+f} = m_3^g + 3m_1^g m_2^f + 3m_2^g m_1^f + m_3^f \tag{8}$$

$$\begin{aligned} m_4^{g+f} &= m_4^g + 4m_1^g m_3^f + 4m_2^g m_2^f + 2m_2^g m_1^f m_1^f \\ &+ 2m_1^g m_1^g m_2^f - 2m_1^g m_1^f m_1^g m_1^f + 4m_3^g m_1^f + m_4^f \end{aligned} \tag{9}$$

Thus, the first four moments for the resultant signal become

$$m_1^{g+f} = 0 \tag{10}$$

$$m_2^{g+f} = \sigma^2 + \frac{nA^2}{2} \tag{11}$$

$$m_3^{g+f} = 0 \tag{12}$$

$$m_4^{g+f} = 3\sigma^4 + 2nA^2\sigma^2 + \frac{3nA^4}{8} \tag{13}$$

The kurtosis for a gaussian distributed signal is given by

$$R = \frac{m_4}{m_2^2} = \frac{3\sigma^4}{(\sigma^2)^2} = 3 \tag{14}$$

In the presence of pulsed-sinusoidal RFI, the moment ratio becomes

$$R = \frac{m_4^{g+f}}{(m_2^{g+f})^2} = \frac{3\sigma^4 + 2nA^2\sigma^2 + \frac{3nA^4}{8}}{\left(\sigma^2 + \frac{nA^2}{2}\right)^2} \tag{15}$$

IV. Blind-spot in detection algorithm

From Eq (15), we see that now the kurtosis ratio depends on thermal power, RFI power as well as the RFI duty cycle. Eq (15) can be re-written as follows

$$R = \frac{m_4^{g+f}}{(m_2^{g+f})^2} = \frac{3P_{th}^2 + 4P_{th}P_{rfi} + \frac{3}{2n}P_{rfi}^2}{(P_{th} + P_{rfi})^2} \tag{16}$$

If the kurtosis ratio becomes 3 then, in spite of the presence of RFI signal, the algorithm will fail to detect it. This indicates a blind-spot in the algorithm. Four conditions are possible for which the kurtosis ratio becomes 3, as follows:

Condition I : $R = 3 \Leftrightarrow n = 0$

Condition II : $R = 3 \Leftrightarrow A = 0$

Condition III: $R = 3 \Leftrightarrow A \neq 0, n = 0.5, \sigma^2 \approx 0$

Condition IV:

$$R = 3 \Leftrightarrow A \neq 0, n \leq 0.5, \quad \frac{P_{th}}{P_{rfi}} = \frac{2\sigma^2}{nA^2} = \frac{|6n-3|}{4n}$$

The first two conditions imply that there is no RFI present, *i.e*. the kurtosis properly equals 3. The third condition is a special limiting case when the duty cycle is 50%. In this case, if the thermal noise is very small compared to the RFI, then the moment ratio will also be 3. The fourth condition, represents a potential blind-spot of the algorithm. If the relationship between the thermal power, RFI power and duty cycle is as shown, then the algorithm will fail to detect RFI. Figure 1 illustrates the relationship between the thermal to RFI power ratio and the duty cycle of the sine pulse under which the algorithm will be blind to the presence of RFI. It is worth noting that practical radars tend to operate with duty cycles well below 50% and so will generally not be subject to this problem.

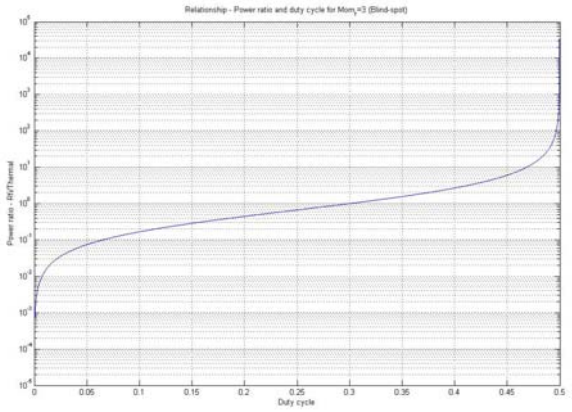

Figure 1. Power ratio vs Duty-cycle for Blind spot

Figure 2. PSR undergoing installation on the WB-57.

V. AIRBORNE FIELD TRIAL

Results of the ADD performance during ground-based field trials have been reported in [6]. A subsequent airborne field trial was performed during August 2005 with the ADD installed in parallel with the standard back-end detector subsystem of the stepped-LO C-Band channel of the NOAA/ETL Polarimetric Scanning Radiometer (PSR). PSR has a programmable AZ/EL positioner that can operate in a number of different scanning modes. A photo of the instrument undergoing installation below the central fuselage of the WB-57 is shown in Figure 2 The ADD was operated during one ~2 hour flight that began and ended near Houston, TX and included overflights of the Dallas-Fort Worth and San Antonio urban areas, more rural portions of east-central Texas, and a brief period out over the Gulf of Mexico. A 60 second sample of the raw measurements while over Dallas is included here, to illustrate ADD performance in the presence of relatively severe levels of RFI. Time/frequency plots of the kurtosis and of the 2nd moment of the measurements are shown in Figures 3 and 4, respectively. In Figure 3, benign, RFI-free, regions are distinguishable by normalized kurtosis values (kurtosis/3) of one. There are two broad regions of the time/frequency space that are free of RFI. They cover frequency channels 171-176 (roughly 7.45-7.50 GHz) during elapsed times 0-25 and 40-50 seconds. Elsewhere, strong excursions from unity of the kurtosis are clearly evident. In figure 4, some of the time/frequency regions with RFI also clearly show spikes of high 2nd moment. RFI in these instances could likely be identified by conventional RFI detection algorithms based solely on the 2nd moment. However, as one counterexample, consider the variations in the 2nd moment at frequency channel 170. The RFI-free elapsed times 0-25 seconds are not noticeably distinguishable from the variations during times 25-40 seconds, when the kurtosis clearly indicates the presence of RFI. A conventional RFI detection algorithm would have considerably more difficulty with this sequence of measurements.

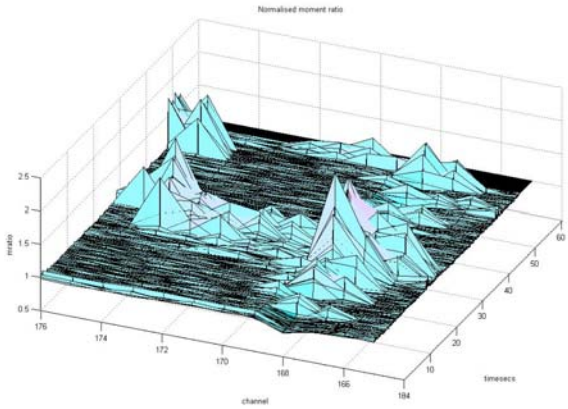

Figure 3. Normalized kurtosis while flying over Dallas. Channel numbers 176-184 roughly correspond to frequencies between 7.4 and 7.5 GHz. The time axis is elapsed time over one minute of data taking. Significant deviations from unity of the normalized kurtosis indicate the presence of RFI.

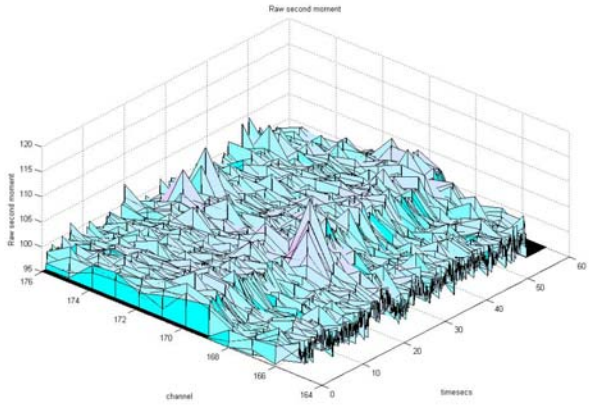

Figure 4. Second moment of measurements during the same period of time as shown in Figure 3. The 2nd moment is linearly proportional to the detected system noise temperature. Spikes in the 2nd moment tend to be associated with the presence of RFI. However, there are time/frequency regions in which the kurtosis clearly indicates that RFI is present but variations in the 2nd moment are not noticeably different from that in regions with variability governed by natural geophysical variability in the observed brightness temperature.

V. CONCLUSIONS

A new type of microwave radiometer detector has been developed that can detect the presence of RFI and, in particular, low level RFI. The Agile Digital Detector directly measures the first four moments of the pre-detected signal, from which the kurtosis of the signal can be computed. In the absence of RFI, the kurtosis is found to be invariant to changes in brightness temperature. In the presence of even very low level pulsed sinusoidal RFI, it changes and, so, can be used to detect its presence. Small variations in the apparent brightness temperature observed – due to low level RFI – that might otherwise be indistinguishable from natural geophysical variability are reliably identified.

ACKNOWLEDGMENTS

The authors would like to acknowledge their collaboration with the NOAA/ETL PSR team, and in particular the assistance of Dr. Albin Gasiewski, during the airborne field trial of ADD. Support for the ADD team was provided by the NASA Goddard Space Flight Center and its Earth Science Technology Office under grants NNG05GB08G and NNG05GL97G. Support for the PSR team was provided in part by the NPOESS Integrated Program Office.

REFERENCES

[1] Li, L., E.G. Njoku, E. Im, P. Change and K. St. Germain, "A preliminary survey of radio-frequency interference over the U.S. in Aqua AMSR-E data," IEEE Trans. Geosci. Remote Sens., 42(2), 380-390, 2004.

[2] Njoku, E.G., P. Ashcroft, T.K. Chan and L. Li, "Global survey and statistics of radio-frequency interference in AMSR-E land observations," IEEE Trans. Geosci. Remote Sens., 43(5), 938-947, 2005.

[3] Le Vine, D.M. and M. Haken, "RFI at L-band in synthetic aperture radiometers," Proc. IGARSS, Toulouse, V. 3, 21-25 July 2003.

[4] Gasiewski, A.J., M. Klein, A. Yevgrafov and V. Leuski, "Interference mitigation in passive microwave radiometry," Proc. IGARSS, Toronto, 2002.

[5] Johnson, J.T., G.A. Hampson, and S. W. Ellingson, " Design and demonstration of an interference suppressing microwave radiometer," Proc. Int. Geosci. Remote Sensing Symposium (IGARSS), Anchorage, Alaska, 2004.

[6] Ruf, C., S.M. Gross, S. Misra, "RFI detection and mitigation for microwave radiometry with an agile digital detector," IEEE Trans. Geosci. Remote Sens., 44(3), 2006.